

## Optical properties of Pr-doped BaY2F8

Adriano B. Andrade, Ana C. S. de Mello, Marcos V. dos S. Rezende, Sonia L. Baldochi, and Mário E. G. Valerio

Citation: *Journal of Applied Physics* **116**, 053521 (2014); doi: 10.1063/1.4892111

View online: <http://dx.doi.org/10.1063/1.4892111>

View Table of Contents: <http://scitation.aip.org/content/aip/journal/jap/116/5?ver=pdfcov>

Published by the [AIP Publishing](#)

---

### Articles you may be interested in

Broadband sensitization of downconversion phosphor YPO<sub>4</sub> by optimizing TiO<sub>2</sub> substitution in host lattice co-doped with Pr<sup>3+</sup>-Yb<sup>3+</sup> ion-couple

*J. Appl. Phys.* **115**, 123103 (2014); 10.1063/1.4869659

BaY<sub>2</sub>F<sub>8</sub> doped with Er<sup>3+</sup>: An upconverter material for photovoltaic application

*J. Appl. Phys.* **114**, 064904 (2013); 10.1063/1.4817171

Structural and optical properties of Pr doped BiFeO<sub>3</sub> multiferroic ceramics

*AIP Conf. Proc.* **1512**, 462 (2013); 10.1063/1.4791111

Synthesis and efficient near-infrared quantum cutting of Pr<sup>3+</sup>/Yb<sup>3+</sup> co-doped LiYF<sub>4</sub> single crystals

*J. Appl. Phys.* **112**, 073518 (2012); 10.1063/1.4757925

Structural and optical properties of europium doped zirconia single crystals fibers grown by laser floating zone

*J. Appl. Phys.* **109**, 013516 (2011); 10.1063/1.3527914

---



**AIP** | Journal of  
Applied Physics

*Journal of Applied Physics* is pleased to  
announce **André Anders** as its new Editor-in-Chief

## Optical properties of Pr-doped BaY<sub>2</sub>F<sub>8</sub>

Adriano B. Andrade,<sup>1,a)</sup> Ana C. S. de Mello,<sup>1</sup> Marcos V. dos S. Rezende,<sup>2</sup> Sonia L. Baldochi,<sup>3</sup> and Mário E. G. Valerio<sup>1</sup>

<sup>1</sup>Physics Department, Federal University of Sergipe, 49100-000 São Cristovão, SE, Brazil

<sup>2</sup>Physics Department, Federal University of Sergipe, 49500-000 Itabaiana, SE, Brazil

<sup>3</sup>IPEN-CNEN/SP, CEP 11049, 05422-970 São Paulo, SP, Brazil

(Received 4 June 2014; accepted 23 July 2014; published online 5 August 2014)

Crystalline samples of Pr-doped BaY<sub>2</sub>F<sub>8</sub> (BaYF) were prepared by zone melting technique. The pure phase obtained was identified by X-ray diffraction measurement. Optical absorption result was evaluated and it showed that the formation of the absorption bands can be connected to color centers generated by radiation in the matrix. Radioluminescence emission measurements after excitation by X-ray showed that the material exhibited components responsible for long lasting phosphorescence. Short decay times were also evaluated, the measurements showed a fast component around 70 ns associated to the 4f<sup>1</sup>5d<sup>1</sup> → 4f<sup>2</sup> transition of the Pr<sup>3+</sup> ion. The Thermoluminescence (TL) results indicate the presence of two trapping centers. © 2014 AIP Publishing LLC.

[<http://dx.doi.org/10.1063/1.4892111>]

### I. INTRODUCTION

Barium yttrium fluoride (BaY<sub>2</sub>F<sub>8</sub>–BaYF) has attracted considerable attention in the last years, particularly when doped with praseodymium, because of its potential use as multiwavelength laser activator for various applications.<sup>1</sup> Recently, BaYF doped with other rare-earth ions was investigated due its scintillator properties,<sup>2</sup> use as a scintillator in radiation detection when doped with Tb<sup>3+</sup> (Ref. 3), and also when doped with Er<sup>3+</sup> and Tm<sup>3+</sup> ions,<sup>4</sup> when doped with Nd<sup>3+</sup> and co-doping Er<sup>3+</sup>, this material has been studied for vacuum ultraviolet (VUV) scintillator applications.<sup>5</sup>

The BaYF has been produced by solid state synthesis and by zone melting technique under reactive atmosphere.<sup>3</sup> The crystal structure is monoclinic, C<sub>2</sub> space group, and the trivalent rare-earth dopant ions are expected to occupy the Y<sup>3+</sup> site.<sup>6</sup> Typical Pr<sup>3+</sup> emission spectra were obtained when Pr<sup>3+</sup> doped BaY<sub>2</sub>F<sub>8</sub> is excited with ionizing radiation or blue light. The spectrum of Pr<sup>3+</sup> doped BaYF presents a wide range of emission in the visible region, with maxima at 483 and 607 nm, corresponding to blue and orange regions in the electromagnetic spectrum. However, the mechanism of light emission of the Pr-doped BaYF is still not explored in the literature. In recent years, fluorides materials doped with Pr<sup>3+</sup> ions have been extensively studied for dosimetric applications,<sup>7</sup> the recombination radiative process and carries trapping for Pr<sup>3+</sup> ion were studied in LiLuF<sub>4</sub> host.<sup>8</sup>

This work is dedicated to the study of the Radioluminescent (RL) spectra of Pr<sup>3+</sup> in the BaYF matrix and the characteristic lifetime of the RL yield aiming the use this system in scintillator devices. Optical absorption (OA) and Thermoluminescence (TL) techniques were also used as additional tools to understand the luminescent mechanism in this material and to follow the radiation damage processes.

### II. EXPERIMENTAL

The pure and doped single crystal was prepared in a platinum reactor from stoichiometric mixture of BaF<sub>2</sub> and YF<sub>3</sub> and with Pr concentrations of 2.0 mol. %. The starting materials were melted at 960 °C under a mixed HF and Argon flow in Pt crucibles. The single crystals were prepared from the synthesized powders by the zone melting method, under a HF atmosphere, in the concentrations of 2.0 mol. % of Pr. Details of the synthesis and the crystals growth can be found in previous work.<sup>9</sup> Powder samples were prepared by grinding the obtained materials in agate mortar.

The crystalline phase was identified by powder X-Ray diffraction measure using Cu K $\alpha$  radiation, operating at 40 kV/40 mA, on a Rigaku RINT 2000/PC diffractometer in the Bragg-Brentano geometry, in the 2 $\theta$  range from 13° to 80° in step scan mode, with steps of 0.02. RL spectra were recorded inside the diffractometer exciting the samples with the same Cu tube. The RL spectra were collected using an optical fiber conducting the light to an Ocean Optics HR2000 spectrometer. The signal decay of scintillation was obtained after excitation by X-ray. The TL measurements were performed from room temperature up to 400 °C using a heating rate linear of 5 °C/s. The light emitted by the sample was detected in two ways: (i) for the sample irradiated with a dose of 0.0924 Gy of X-ray, the TL was collected using a standard photomultiplier tube (EMI 9789-B) fed by a variable high voltage source; (ii) for the samples heavily irradiated with doses of 431 Gy of  $\beta$  rays, the TL emission was taken by an optical fiber coupled to a Ocean Optics Maya 2000 spectrometer. With this latter arrangement, it was possible to obtain a complete set of emission spectra as the samples were heated up inside the TL apparatus. Since all samples were powders, the OA spectra were obtained via diffuse reflectance using a polychromatic light source (Mikropack DH-2000 UV-Vis-NIR) and an optical fiber attached to an Ocean Optics HR2000 spectrometer. The lifetime measurements were measured at the X-ray absorption

<sup>a)</sup>abandrade1@gmail.com

fine structure (D08B-XAFS-2) beamline of the Brazilian Synchrotron Light Laboratory (LNLS) source in Campinas, Sao Paulo, Brazil, using the single-bunch mode, with X-ray pulse intervals of 311 ns and pulse FWHM of about 100 ps. A HAMAMATSU R928 photomultiplier (PMT) directly connected to a 3.5 GHz bandwidth, 40 GSa/s WavePro 735Zi, Teledyne LeCroy oscilloscope. The light pulse was collected in the PMT and the current pulse was connected in one of the oscilloscope channels, using the 50  $\Omega$  internal resistance load. The second channel of the oscilloscope was connected to the square wave trigger signal coming from the synchrotron storage ring, used to synchronize the light pulse with the electrons bunch in the ring. With this arrangement the time resolution was estimated to be around 8–10 ns.

### III. RESULTS AND DISCUSSION

Powder XRD results of the samples are shown in Fig. 1, as compared to the Guilbert *et al.*<sup>10</sup> standard diffraction pattern. The diffraction peaks in Fig. 1 can be indexed to the monoclinic phase structure of BaYF with no extra peaks related to other phases. Also, for the Pr-doped sample, there is no evidence of any other phases, indicating that the doping with Pr (2% mol) ions has nearly no effect on the phase formation. A small amount of Pr into BaYF will not change the host structure due to the similar ionic radii of Pr<sup>3+</sup> (0.99 Å) and Y<sup>3+</sup> (0.90 Å).<sup>11</sup> Previous results from atomistic simulations reported that in BaYF structure Pr<sup>3+</sup> can occupy the Y<sup>3+</sup> sites inducing only a distortion of the local symmetry of the active ion,<sup>6</sup> as compared to the original Y<sup>3+</sup> environment.

The radiation damage is observed in the Pr-doped BYF when irradiated with X-ray and this effect manifested as changes in the scintillation efficiency, this can be to trapping of the free carrier in electrons and holes center.<sup>12</sup> Also, it was observed that the irradiated regions of the samples have different coloration. In order to understand this behavior, the intensities of optical absorption bands generated by the X-rays were followed as a function of dose. The reflectance spectra were measured for virgin Pr doped samples and for irradiated samples different doses, varying from 0.924 to 2.772 Gy. Optical absorption spectra of the samples were measured from the reflectance spectra assuming that no light is transmitted through the powder samples and that was

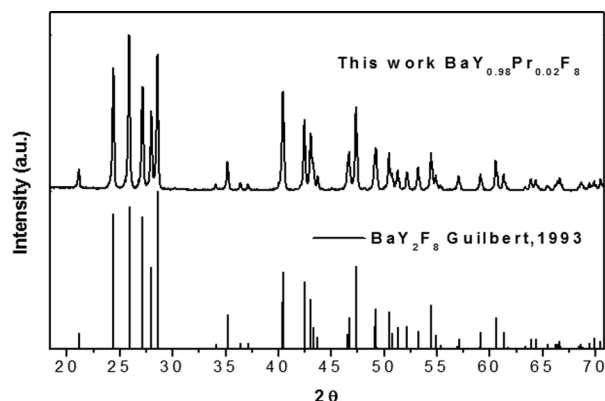


FIG. 1. XRD powder pattern of the single crystalline sample of BaYF:Pr<sup>3+</sup>. The peaks were identified to the BaY<sub>2</sub>F<sub>8</sub><sup>10</sup> standard patterns.

assured by using a large amount of powder deposited on a reflective white Teflon surface. The OA spectra are given in Figs. 2(a) and 2(b).

For non-irradiated Pr-doped samples, three weak absorption bands are observed at 445, 460, and 597 nm, these bands can be attributed to the Pr<sup>3+</sup> transitions between the <sup>3</sup>H<sub>4</sub> ground state and the <sup>3</sup>P<sub>2</sub>, <sup>3</sup>P<sub>1</sub> + <sup>3</sup>P<sub>0</sub>, and <sup>1</sup>D<sub>2</sub> states, respectively.<sup>13</sup> When the samples were irradiated with different doses, the optical absorption intensity increased. No apparent changes in the position of the Pr<sup>3+</sup> peaks were observed as the doses increased. The main changes are related to the appearance of additional absorption bands centered at about 300, 500, 600, and 800 nm in the sample. These wide bands are formed by the superposition of the bands attributed to Pr ion and the absorption band due to defects centers generated by irradiation. In the previous works,<sup>2</sup> absorption band at about 300 and 800 nm due to the radiation induced color centers were also observed and it was shown that they are independent of doping ion. These additional bands are directly linked to the BaYF structure. The most probable defects in fluorides are F-type centers F, F<sup>-</sup>, or FA centers, i.e., electrons localized in anion vacancies, and modified V<sub>k</sub> centers formed by a pair of fluorine ions that traps a hole forming F<sup>-2</sup> type molecule. All these defects are known to produce absorption bands in the 240–380 nm, 300–330 nm, 450–600 nm, and 790–830 nm regions in other fluoride matrices.<sup>14,15</sup>

In Fig. 3, a typical RL emission spectra is shown with the dependence of the intensity of the two main emission peaks at 483 nm (<sup>3</sup>P<sub>1</sub> + <sup>1</sup>I<sub>6</sub> → <sup>3</sup>H<sub>4</sub>) and 607 nm (<sup>1</sup>D<sub>2</sub> → <sup>3</sup>H<sub>4</sub>) as function of the dose deposited in the samples. The darkening of Pr doped BaYF sample is observed after irradiation. This behavior also is observed when the BaYF are doped with the other rare earth dopant<sup>2,4</sup> and these results are consistent with the dependence of the OA with the irradiation dose, indicating that the color change is related to the OA bands induced by irradiation. This results can be explain for trapping of the pairs electron-hole in intrinsic defects Frenkel anionic and cationic, when free carrier are trapping during irradiation on color centers, in this case, F and V<sub>k</sub> centers.<sup>14</sup>

Fig. 4 shows the RL intensity and absorption bands attributed to radiation damage in function of the absorbed

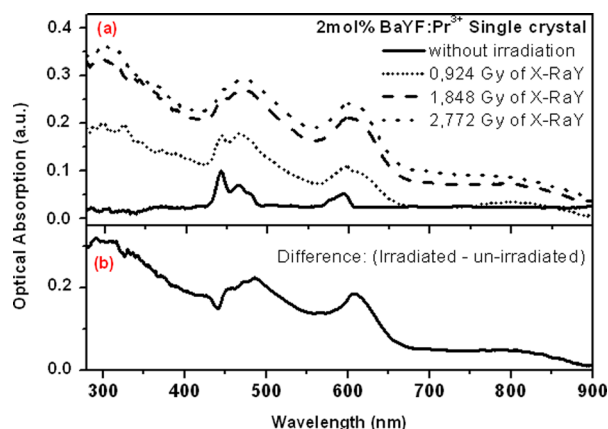


FIG. 2. (a) OA spectra of Pr-doped BaYF single crystals samples irradiated with different doses of X-rays. (b) Difference between the OA spectra of the un-irradiated and the OA spectra of the sample irradiated with 1.848 Gy.

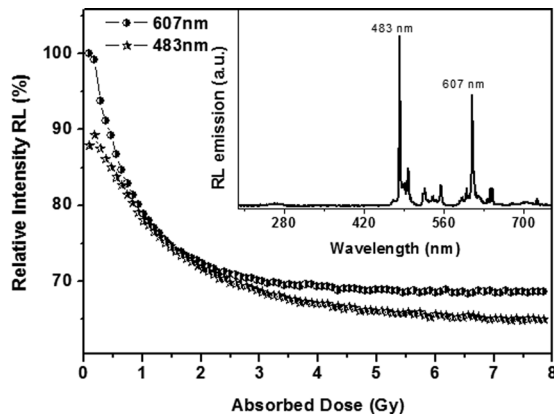


FIG. 3. Intensity of the emission peak at 483 nm and 607 nm as a function of the X-ray absorbed dose.

dose, which is responsible for the color centers formation. When the absorbed dose increase, the irradiation induces the creation of defects in the lattice that could be related to the F-type centers ( $F$ ,  $F^-$ , or  $F_A$  centers) and modified  $V_k$ . From Fig. 4, it can be seen that intensity of the absorption bands centered at 483 nm and 607 nm increasing as a function with the absorbed dose and, in the other hand, the RL intensity of the at 483 nm and 607 nm transitions decreasing. In this case, this behavior is attributed to the self-absorption, where the RL emission is absorbed to the sample, contributing to the change of scintillation efficiency.

In order to investigate further the effect of the  $Pr^{3+}$  doping on the RL yield, TL was carried out aiming the identification of charge traps. The TL glow curves of the pure and  $Pr^{3+}$  doped  $BaYF$  single crystals were obtained after irradiating the samples with a dose of 0.0924 Gy of X-rays (see Fig. 5). In the pure single crystals, a main TL peaks at 123 °C was observed, while for the  $Pr^{3+}$  doped  $BaYF$ , the TL presented two main peaks, at 105 °C and 184 °C. The results indicated that the  $Pr^{3+}$  dopant has some effect on the distribution of charge trapping states in the  $BaYF$  matrix. The main peak at 123 °C for the pure sample is asymmetrical, having a typical first order peak shape. The peak at 105 °C for the doped sample looks symmetric indicating that either the mechanism changed from first order to second order,<sup>16</sup> as compared to pure  $BaYF$  sample, or this 105 °C TL peak is a

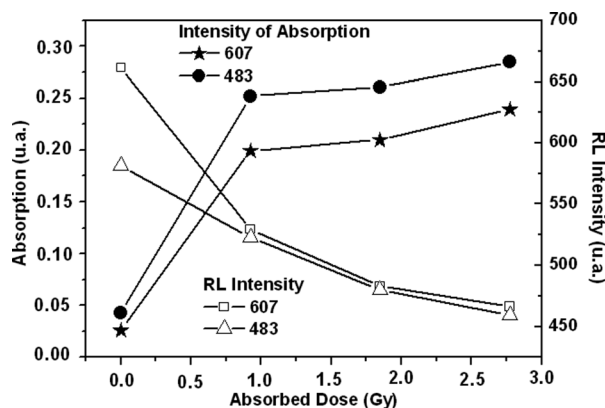


FIG. 4. RL emission peak intensities and optical absorption intensities at 483 nm and 607 nm as a function of the X-ray absorbed dose.

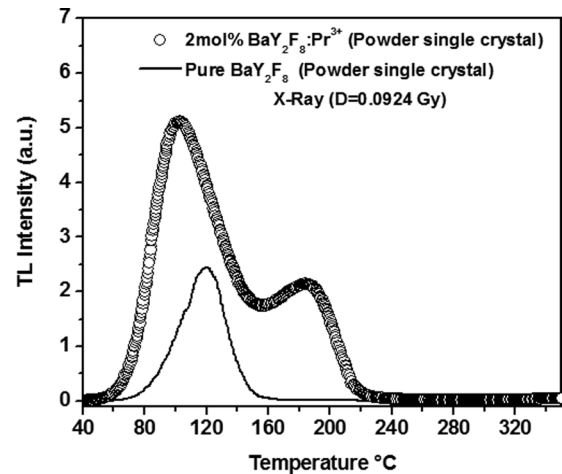


FIG. 5. Thermoluminescence glow curves of powders of the pure single and doped  $BaYF:Pr^{3+}$  single crystal irradiated with 0.0924 Gy of X-rays.

superposition of a lower temperature peak and the 123 °C peak from the  $BaYF$  matrix. Since the presence of the defect is able to stabilize new trapping centers, as indicated by the presence of the 184 °C TL peak in the doped sample, it is likely that the second option is what is happening, more detailed studies are required for a better understanding.

Fig. 6 shows typical emission spectra of  $Pr$  doped  $BaYF$  TL peak at 105 °C irradiated with 341 Gy of  $\beta$  radiation. It has been observed that fluoride crystals doped with praseodymium has the ability to absorb large amounts of beta radiation, up to dose of  $8 \times 10^3$  Gy.<sup>7,8</sup> The emission spectra showed in Fig. 6 are formed by quite sharp peaks characteristic 4f–4f transitions from the  $^3P_1$  level of the  $Pr^{3+}$  ions.<sup>7,17</sup> All main transitions were identified and they are as follows:  $^3P_1 + ^1I_6 \rightarrow ^3H_4$  (478 nm),  $^3P_2 \rightarrow ^3H_5$  (491 nm),  $^3P_1 + ^1I_6 \rightarrow ^3H_5$  (520 nm),  $^1D_2 \rightarrow ^3H_4$  (607 nm),  $^3P_2 \rightarrow ^3F_4$  (640 nm), and  $^1D_2 \rightarrow ^3H_4$  (681 nm). The results observed in Fig. 6 show that the TL emission center is the  $Pr^{3+}$  ions and during the TL processes the recombination of the trapped charges excite the  $Pr^{3+}$  ions, as noted by Kristianpoller *et al.*<sup>7</sup> and Voronova *et al.*<sup>8</sup> in other fluoride materials.

Fig. 7 shows the scintillation decay time of the  $Pr$  doped  $BaYF$  sample measured in single-bunch mode at the XAFS2

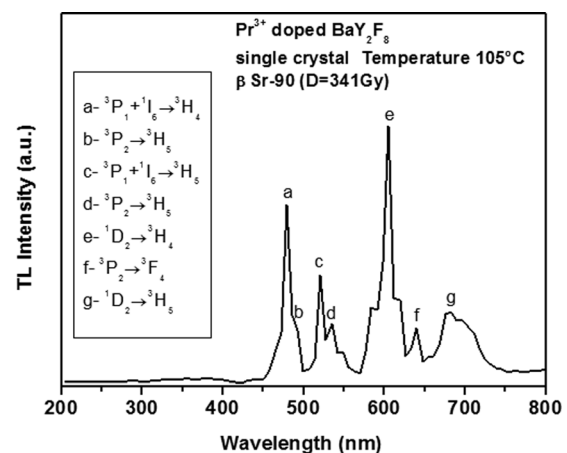


FIG. 6. Typical emission spectra of the 105 °C TL peak, showing the characteristics transitions of  $Pr^{3+}$ .

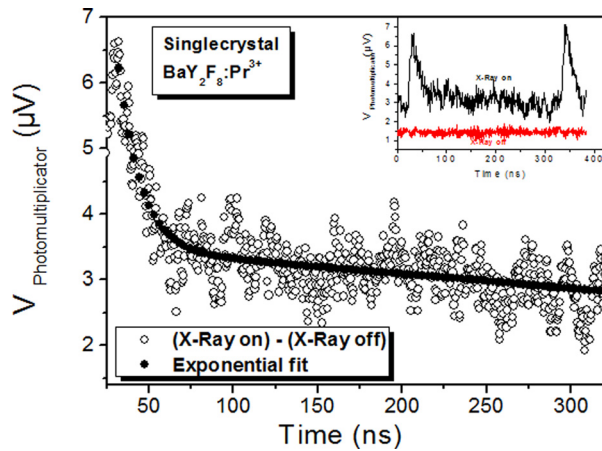


FIG. 7. RL time decay of the Pr doped BaYF sample excited with 5247 eV X-ray photon pulses.

beamline of the Brazilian Synchrotron Light Laboratory (LNLS) using excitation energy of 5247.0 eV, at the Ba  $L_{III}$  absorption edge. The decay curve was fitted to a bimodal exponential decay model, according to the following equation:

$$I(t) = I(\infty) + A_1 e^{-x/t_1} + A_2 e^{-x/t_2}, \quad (1)$$

here  $I(t)$  represent the luminescence intensity at a time “t” after the X-ray pulse,  $I(\infty)$  represents the intensity of the luminescence that did not decay in the time interval between X-ray pulses,  $A_1$  and  $A_2$  represent the relative intensities of each component, and  $t_1$  and  $t_2$  are the characteristic decay time of the two processes. The fitting results are shown in Table I. Two constants time of decay were found,  $(13 \pm 2)$  ns and  $(70 \pm 5)$  ns. The first value is very close to the time resolution of our detection system ( $\sim 10$  ns) and it is probably related to the response time of the electronics associated to the detection. The second time, however, can be associated to the relaxation of the  $\text{Pr}^{3+}$  ions from the  $4f^1 5d^1$  excited states back to the  $4f^2$  ground states.<sup>18,19</sup> This value is very close to others values found in the literature for that  $\text{Pr}^{3+}$  transitions and these transitions can be quite fast because they are electric dipole allowed transitions.<sup>19</sup>

Fig. 7 also shows that part of the emission did not decay in the interval between pulses. This slow component is characterized by  $I(\infty)$  and it represents around 60% of the total luminescent signal. This slow component can be connected to two main sources. One of them is related to the typical  $4f-4f$  transition time of all trivalent rare-earth ions that are much greater than 311 ns, the time window between two X-ray pulses, electric-dipole  $4f-4f$  transitions of lanthanide ions such as  $\text{Pr}^{3+}$ ,  $\text{Eu}^{3+}$ , and  $\text{Tb}^{3+}$ , are parity forbidden and hence slow ( $\sim 0.01-1$  ms).<sup>20</sup> The other possible source for the slow component could be related to the presence of

TABLE I. Fit parameters for the RL time decay curve shown in Fig. 7.

Pr doped BaYF	$I_i(\infty)$ (%)	Time (ns)	Total (%)
1st process	60	$\sim 13$	38
2nd process		$\sim 70$	2

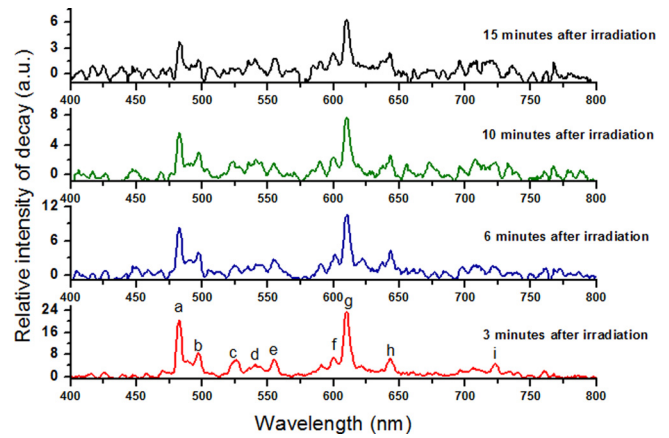


FIG. 8. Phosphorescence emission after X ray irradiation.

shallow traps that can trap the charge carriers generated during the excitation pulse, delaying the recombination between the electrons and holes. The energy released due to the electron-hole pair recombination can excite the  $\text{Pr}^{3+}$  ions directly to the  $4f5d$  configuration giving rise to the series of emission peaks due to the dopant ion.

The emission spectrum of Pr doped BaYF was also recorded after stopping the X ray excitation and the results were shown in Fig. 8. The emission peaks are similar to the ones observed for the emission spectra of TL peak at  $105^\circ\text{C}$  (see Fig. 6). These results are evidence that trapped charges are recombining and transferring the energy to the  $\text{Pr}^{3+}$  ions.<sup>7,8,21</sup> In Fig. 8, the intensities of the emission peaks decreased because the number of trapped electrons and holes also decreased as the time after ceasing irradiation.

The peaks observed in Figs. 6 and 8 that can be assigned to the  $4f-4f$  transitions of  $\text{Pr}^{3+}$  ions were listed in Table II. The identification of the transitions were based on data from the literature concerning the  $\text{Pr}^{3+}$  emission spectra in fluorides host lattices.<sup>7,17,22</sup>

Based on all results discussed previously, it is possible to propose a scintillation mechanism for the Pr doped BaYF. The first step involves the relaxation of the initial electronic excitation, where the absorption of a high-energy photon creates an inner shell hole and an energetic primary electron following by the thermalization of the hot electrons and holes by intra band transitions and electron-phonon relaxation bringing the electrons to the bottom of the conduction band and the holes to the top of the valence band. At least two

TABLE II. Emission lines attribution in  $\text{Pr}^{3+}$  doped  $\text{BaY}_2\text{F}_8$ .

Lines	Wavelength (nm)	Transitions
a	482	$^3P_1 + ^1I_6 \rightarrow ^3H_4$
b	497	$^3P_2 \rightarrow ^3H_5$
c	526	$^3P_1 + ^1I_6 \rightarrow ^3H_5$
d	542	$^3P_2 \rightarrow ^3H_6$
e	556	$^3P_2 \rightarrow ^3H_6$
f	600	$^1D_2 \rightarrow ^3H_4$
g	607	$^1D_2 \rightarrow ^3H_4$
h	644	$^3P_2 \rightarrow ^3F_4$
i	722	$^1D_2 \rightarrow ^3H_5$

possible routes can be followed after this first stage. The electrons and holes recombine via intra-band transitions and photons are produced (path 1). The other possibility is that part of the electrons and holes can be trapped in trapping centers in the forbidden gap. These trapped charges can stay in these trapping centers for short or long periods depending on the trap depth and the de-trapping probability constant. The ones that stayed trapped for longer times will give rise to the TL emission upon heating up of the sample (path 2) and the ones that are released from the traps within shorter intervals can give rise to the delayed luminescence (path 3), also known as afterglow. In the next stage, the photons generated due to the recombination between the electrons and holes, either directly via path 1 or path 2, can excite the luminescence centers that relax back to their ground state by emitting the characteristic luminescence.<sup>7,8,21</sup> In the Pr doped BaYF, these photons generated due to the electron-hole recombination will have energies around at least 10 eV, due to the large band gap of the fluorides.<sup>23,24</sup> This energy is enough to excite the Pr<sup>3+</sup> ions from the 4f<sup>2</sup> ground states to the 5d<sup>1</sup>4f<sup>1</sup> excited states. And the excitation happens both during the irradiation giving rise to the radioluminescence light yield or during the TL emission and that is why both emission spectra are very similar.

#### IV. CONCLUSIONS

In this paper, we have presented results of BaY<sub>2</sub>F<sub>8</sub>:Pr<sup>3+</sup> single crystal growth by the zone melting method. The optical absorption of the X-ray irradiated samples were monitored as a function of the dose. In non-irradiated Pr doped sample, two weak absorption bands are observed and attributed to the Pr<sup>3+</sup> transitions from the <sup>3</sup>H<sub>4</sub> ground state to the <sup>3</sup>P<sub>2</sub>, <sup>3</sup>P<sub>1</sub> + <sup>3</sup>P<sub>0</sub>, and <sup>1</sup>D<sub>2</sub> states. The exposure to prolonged X-ray irradiation induces two additional absorption bands in the sample. The radiation damage of Pr doped BaYF samples was observed and it was found to be roughly independent on the dopant ions. RL emission spectra showed the <sup>3</sup>P<sub>1</sub> + <sup>1</sup>I<sub>6</sub> → <sup>3</sup>H<sub>4</sub> (483 nm) and <sup>1</sup>D<sub>2</sub> → <sup>3</sup>H<sub>4</sub> (607 nm) transitions as a function with the absorbed dose and their intensities were monitored. The results showed that the x-ray irradiation induces the creation of the defects in the lattice. The TL results indicated that two additional peaks (105 °C and 184 °C) in the doped samples can be ascribed to the presence of either electron or hole traps (or both) in the energy gap of the host. The RL life time was also measured using single bunch mode of synchrotron radiation at the LNLS, and the results revealed that the Pr doped BaYF has two decay time constants, one of them, τ<sub>1</sub> = (13 ± 2) ns, is due to the time response of the detection system and the other one,

τ<sub>2</sub> = (70 ± 5) ns, was attributed to the 4f<sup>1</sup>5d<sup>1</sup> → 4f<sup>2</sup> transitions that are electric dipole allowed. The 105 °C TL spectrum emission showed the characteristic lines of the Pr<sup>3+</sup> ion and the last long phosphorescence can be due to the slow electron-hole pair recombination after irradiation.

#### ACKNOWLEDGMENTS

The authors gratefully acknowledge the CAPES, CNPq, FAPITEC/SE and FAPESP for financial support. Synchrotron radiation measurements were done at the LNLS—Brazilian Synchrotron Light Laboratory/MCT under Proposal XAFS No. 9358/10.

- <sup>1</sup>R. Piramidowicz, R. Mahiou, P. B. Boutinaud, and M. Malinowski, *Appl. Phys. B* **104**, 873 (2011).
- <sup>2</sup>A. C. S. Mello, A. B. Andrade, G. H. G. Nakamura, S. L. Baldochi, and M. E. G. Valerio, *Opt. Mater.* **32**, 1337 (2010).
- <sup>3</sup>M. E. G. Valerio, V. G. Ribeiro, A. C. S. Mello, M. A. C. Santos, S. L. Baldochi, V. L. Mazzocchi, C. B. R. Parente, R. A. Jackson, and J. B. Amaral, *Opt. Mater.* **30**, 184 (2007).
- <sup>4</sup>A. C. S. Mello, A. B. Andrade, G. H. G. Nakamura, S. L. Baldochi, and M. E. G. Valerio, *J. Lumin.* **138**, 19 (2013).
- <sup>5</sup>J. Pejchal, M. Nikl, K. Fukuda, N. Kawaguchi, T. Yanagida, Y. Yokota, A. Yoshikawa, and V. Babin, *Radiat. Meas.* **45**, 265 (2010).
- <sup>6</sup>J. B. Amaral, M. A. C. Santos, M. E. G. Valerio, and R. A. Jackson, *Appl. Phys. B* **81**, 841 (2005).
- <sup>7</sup>N. Kristianpoller, D. Weiss, N. Khaidukov, V. Makhov, and R. Chen, *Radiat. Meas.* **43**, 245–248 (2008).
- <sup>8</sup>V. Voronova, N. Shirana, A. Gektin, V. Nesterkina, K. Shimamura, and E. Villora, *Radiat. Meas.* **42**, 823 (2007).
- <sup>9</sup>S. F. A. Cruz, Ph.D. Thesis, University of São Paulo, São Paulo, 2008.
- <sup>10</sup>L. H. Guilbert, *Mater. Res. Bull.* **28**, 923 (1993).
- <sup>11</sup>R. D. Shannon, *Acta Crystallogr., Sect. A* **32**, 751 (1976).
- <sup>12</sup>C. Greskovich and S. Duclos, *Annu. Rev. Mater. Sci.* **27**, 69 (1997).
- <sup>13</sup>L. R. Moorthy, T. S. Rao, K. Janardhanam, and A. Radhapathy, *J. Alloys Compd.* **298**, 59 (2000).
- <sup>14</sup>G. M. Renfro, J. C. Windscheif, and W. A. Sibley, *J. Lumin.* **22**, 51 (1980).
- <sup>15</sup>S. M. Kaczmarek, A. Bensalah, and G. Boulon, *Opt. Mater.* **28**, 123 (2006).
- <sup>16</sup>M. Keever, *Thermoluminescence of Solids* (Cambridge University Press, 1983).
- <sup>17</sup>A. A. Kaminskii, *Crystalline Lasers, Physical Process and Operating Schemes* (CRC-press, 1996).
- <sup>18</sup>A. S. Potapov, P. A. Rodnyi, S. B. Mikhrin, and I. R. Magunov, *Phys. Solid State* **47**, 1436 (2005).
- <sup>19</sup>M. Sugiyama, T. Yanagida, Y. Yokota, S. Kurosawa, Y. Fujimoto, and A. Yoshikawa, *Radiat. Meas.* **55**, 112 (2013).
- <sup>20</sup>M. J. Weber, *Nucl. Instrum. Methods Phys. Res., Sect. A* **527**, 9 (2004).
- <sup>21</sup>J. Marczazzo, M. Santiago, E. Caselli, N. Nariyama, and N. M. Khaidukov, *Opt. Mater.* **26**, 65 (2004).
- <sup>22</sup>B. Di Bartolo and B. E. Bowlby, *J. Lumin.* **102–103**, 481 (2003).
- <sup>23</sup>E. Sarantopoulou, Z. Kollia, and A. C. Cefalas, *Microelectron. Eng.* **53**, 105 (2000).
- <sup>24</sup>E. Sarantopoulou, Z. Kollia, A. C. Cefalas, V. V. Semashko, R. Yu. Abdulsabirov, A. K. Naumov, S. L. Korableva, T. Szczurek, S. Kobe, and P. J. McGuinness, *Opt. Commun.* **208**, 345 (2002).